45TH TURBOMACHINERY & 32ND PUMP SYMPOSIA
HOUSTON, TEXAS | SEPTEMBER 12 – 15, 2016
GEORGE R. BROWN CONVENTION CENTER

SUBSYNCHRONOUS VIBRATIONS ON TURBOEXPANDERS EQUIPPED WITH MAGNETIC BEARINGS ASSESSMENT, UNDERSTANDING AND SOLUTIONS

Houman Shokraneh, Ph.D.
Director of Engineering
L.A. Turbine (LAT)
Valencia, California, USA

Laurent Richaume
Rotating Equipment Engineer
TOTAL E&P
Pau, France

Bernard Quoix
Head of Rotating Machinery Department
TOTAL E&P
Pau, France

Matthieu Oliva
Technical Support Manager
SKF Magnetic Mechatronics (S2M)
France

Houman Shokraneh, Ph.D. *is Director of Engineering at L.A. Turbine (LAT). Since joining the company in 2008, his responsibilities include supervising LAT's global engineering team, defining R&D projects and implementing new ideas in turboexpander design. His achievements include designing more than one hundred unique turboexpander units currently in operation throughout the world. Dr. Shokraneh received his B.S. degree (Aerospace and Mechanical Engineering, 1999) from Sharif University of Technology, M.S. degree (Mechanical Engineering, 2003) and Ph.D. degree (Mechanical Engineering, 2007) from the University of Southern California. He is a member of ASME.*

Laurent Richaume *is a Rotating Equipment Engineer for TOTAL E&P, in Pau, France. He joined TOTAL in 2014, and he is involved in projects requiring turbomachines such as compressors, gas turbines, pumps, and expander-compressors. He also supports site activities. Laurent Richaume graduated from INSA (Institut National des Sciences Appliquées) in Toulouse (France) in 1994. He began his career in 1995, working as a rotating equipment engineer for Gaz De France, a national gas transportation company. Then from 2005 until 2014 he joined the rotating equipment department of Air Liquide Engineering, being head of this department from 2011 until 2014. He joined TOTAL in 2014 at Rotating Machines Department.*

Bernard Quoix *is the Head of TOTAL E&P Rotating Machinery Department since November 2003. He started his career in 1979 within TOTAL Operations in the North Sea, then from 1986 to 1989 became Head of Engineering of Turbomeca Industrial Division, then went to Renault Car Manufacturer as Assistant Manager of the engine testing facilities, before joining Elf Aquitaine and eventually TOTAL, mainly involved in all aspects of turbomachines and bringing his expertise to Operations of all TOTAL Affiliated Companies worldwide. Bernard Quoix graduated from ENSEM (Ecole Nationale Supérieure d'Electricité et de Mécanique) in Nancy (France) in 1978 and then completed his engineering education with one additional year at ENSPM in Paris, specializing in Internal Combustion Engines. He is a member of the Turbomachinery Advisory Committee since 2005. He is also the President of ETN (European Turbine Network), an organization based in Brussels, since 2010.*

Matthieu Oliva *is Technical Support Manager at SKF Magnetic Mechatronics (S2M). He joined S2M in 2006 and has held a variety of different positions related to magnetic bearing technology. He holds an engineering degree from École Centrale Paris.*

ABSTRACT

In most natural gas applications, turboexpanders are operating close to or on the dew point line and a mixture entering the turboexpander impeller is a combination of liquid and gas phases of the natural gas. The presence of the liquid phase may induce rotordynamic instabilities during operation. Special care should be taken in the case of magnetic bearings.

This paper will present a revamp of two turboexpander-compressors equipped with active magnetic bearings (AMB). The application is liquid natural gas (LNG) rejection and gas injection on a Floating Production, Storage and Offloading (FPSO) barge. Prior to upgrade, the turboexpanders had accumulated more than 250 thousand hours in operation. The objective of the upgrade was to adapt to new process conditions and to increase the power of the turboexpanders. After the re-wheeling of turboexpanders, numerous trips due to violent subsynchronous vibrations were experienced. The root-cause analysis revealed that the presence of liquids in the front wheel labyrinth seals caused fluid-induced non-synchronous vibrations (NSV). Methods used in the redesign of the impellers and labyrinth seals that allowed the problem to be solved will be described in detail.

BACKGROUND

TOTAL has operated N'Kossa field since 1996. Facilities developed to operate this plant comprise a FPU and two satellites platforms. Valenchon, C et al. (1995) detailed the main characteristics of the concrete barge itself and its production capacity.

Two identical turboexpander-compressors were put into operation in 1996 for LNG rejection and gas injection applications (Table 1). The AMB were based on a field-proven standardized design used in a number of turboexpanders in this power range. Details can be found in (Agahi, et al., 1995). By 2013, the two units had accumulated more than 250 thousand hours of operation. The documented availability of AMB was 99.95% (Bloch and Soare, 2001).

In 2010, after almost 15 years of operation, additional gas volume to be processed by the expander-compressors required a complete re-staging of this equipment. Expander inlet pressure was reduced down to 79 bar Abs (original design was 82 bar Abs), with an outlet pressure of 26 bar Abs and the mass flow expanded was increased from 55 to 63 kg/sec. The volume flow to be processed through this expander-compressor was increased by almost 20% (Table 1).

This additional gas flow to be processed required a complete redesign of both the expander and compressor impellers. This re-staging also presented the opportunity to upgrade the active magnetic bearing control cabinet. The original analog control cabinet E120V/30-60 Amps was replaced by a modern digital model E160/60. The original bearing design was still suitable with the updated design of the shaft, taking into account the new shaft and the larger and heavier impellers. The complete rotordynamic analysis confirmed the feasibility and conformity to API 617 standards.

Figure 1: N'Kossa is an oil, gas and condensate field production, located 60 km offshore Pointe-Noire, Congo

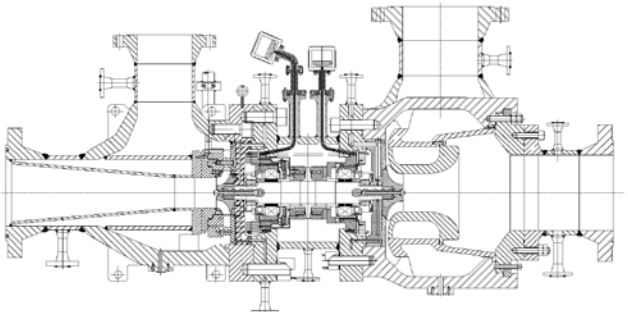

Figure 2:Turboexpander with magnetic bearing cross-section

Following successful Factory Acceptance Tests (FAT), commissioning and start-up of these upgraded expanders took place in early 2013. When the expander reached 15,000 RPM (250 Hz), a high level subsynchronous vibration, around 100 Hz, was detected. The rotor displacement due to these forced vibrations reached the trip threshold set at 90 µm and the unit was not able to be operated at a higher rotating speed. Several attempts to speed-up the unit above the 15,000 RPM limit failed, as the unit tripped systematically.

The magnetic bearings alarm/trip thresholds for the shaft displacement are related to the minimum air gap at back-up bearings and usually set at roughly 40%-60% of the nominal gap value. This is done in order to prevent any physical contact between rotor and stator. It should be noted that during trips the rotor remains levitated and no landing on back-up bearings occurs.

	Original	First Redesign
Rated power	3.7 kw	3,7 kw
Nominal speed	21,000 RPM	21,000 RPM
Expander wheel – mass/diameter	4.8 kg/239 mm	7.7 kg/239 mm
Compressor wheel – mass/diameter	7 kg/300 mm	11.1 kg/300 mm
Wheel material	AL 6061	TI – Grade 29
Wheel type	Shrouded	Shrouded
Equipped rotor mass	106 kg	113.2 kg
Radial AMB diameter	150 mm	
Max radial AMB load	4,700 N	
Axial bearing diameter	279 mm	
Max axial AMB load	22,000 N	
Radial gap at auxiliary bearings	150 µm	
Radial displacement Alarm/Trip set points	60 µm / 90 µm	
Pressure /Temperature - Expander inlet	81.9 bar/-9° C	79 bar /-5.6° C
Pressure /Temperature - Expander outlet	27 bar/-55.9° C	26 bar /-55.6° C
Pressure /Temperature - Compressor inlet	24.7 bar /26° C	22.9 bar /14.6° C
Pressure/Temperature - Compressor outlet	37.3 bar/60.6° C	36.1 bar /53.8 °C

Table 1: Wheel and bearing design properties

The results of the root cause analysis (RCA) are described below.

FIRST REDESIGN (SHROUDED WHEEL)

This machine is located on an offshore platform, so one of the constraints was to minimize the changes and the amount of rework performed on these units. In order to reduce the amount of rework, the diameter of the redesigned wheels had to be kept the same as the original design. To accommodate the higher flow, the nozzle thickness increased and blade angles changed to open up the area. On the original design, both wheels (expander and compressor) were made out of Al 6061 and they did not have any surface coating to protect them from corrosive components. Overtime, because of an increase in the amount of mercury in the process gas, several failures were observed on the impellers which were due to corrosion attack that occurred between 1998 and 2010. During the redesign process, the wheel material was changed to TI grade 29, a more mercury-resistant material that would prevent future impeller corrosion and damage.

To have a rotordynamics acceptable behavior with these heavier wheels, the weight, center of gravity and momentum of inertia of both expander and compressor wheels had to be kept as close as possible to the original Aluminum wheel design. Combined FEA and CFD analysis provided the opportunity to find the optimum point for the redesign without sacrificing efficiency. Rotordynamics studies, performed by the original magnetic bearing supplier, confirmed that the newly designed wheels could be mounted on the original rotor-bearing assembly and meet the API 617 rotordynamics criteria.

The newly designed units were installed on April 2013. During the initial start-up of Unit A, the machine tripped (hard landing) at around 15,000 RPM. Several attempts to bring the unit speed up were performed after the initial start-up, but they were all unsuccessful with the unit tripping at 13,000-17,000 RPM depending on the operating conditions.

Different discharge pressures and inlet guide vane (IGV) openings were tested and at no time could the unit run higher than 17,000 RPM. Subsynchronous vibration was showing up in all configurations after 13,000 RPM and the main reason for the unit trip was excessive radial vibration on the expander bearing. When the discharge pressure increased from 26 to 29.5 bar the subsynchronous vibration appearance moved from 13,000 to 15,000 RPM and the unit could speed up to 17,000 RPM (Figure 3).

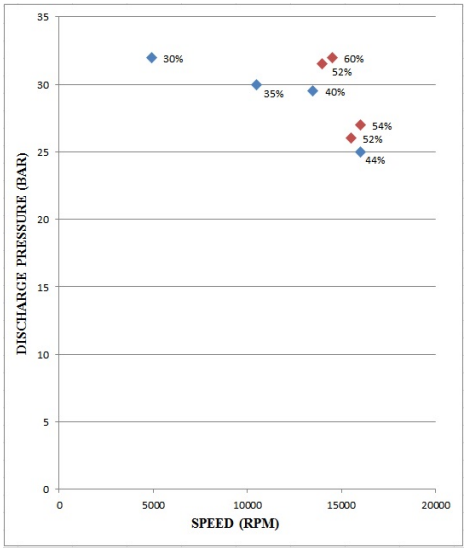

Figure 3: Discharge pressure vs Speed for each IGV position

To evaluate the effect of the temperature, several inlet conditions were considered. When the expander start-up took place with the inlet temperature in the lower part of the design range (-11°C), subsynchronous vibration inception occurred very quickly during the sequence around 13,000 RPM. On the opposite, when the start-up sequence took place with the inlet temperature in the warmer range (-5°C), subsynchronous vibration appeared at a higher speed, around 15,000 RPM, but it was never possible to go beyond 17,400 RPM. It was also noticed that when the IGV is fully open (throttling with upstream valve), the subsynchronous forced vibrations appeared at the same speed as before but with much lower amplitude (Figure 4).

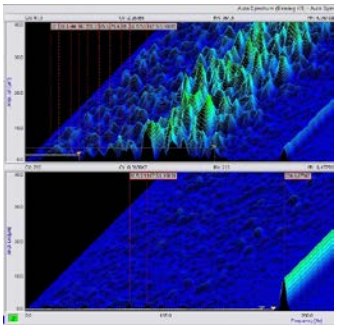

Figure 4: FFT for 15,000 RPM
Top: Expander, Bottom: Compressor

It was clear at this point that non-synchronous vibration (NSV) was a function of the operating gas conditions (pressure and temperature) and IGV position (IGV position dictates flow and pressure after the nozzles).

The magnetic bearing control system provides a powerful tool for monitoring and diagnostics, allows performing detailed analysis of vibrations, including vibration spectrum, orbits and waterfalls. This was made possible thanks to an in-build data logger that registers high-resolution (14 kHz) data during trips and low-resolution (1 Hz) during normal operation. Below are results of an analysis of the recovered data. The position spectrum may be compared between the rotation speed of 150 Hz and 230 Hz:

- For frequencies higher than 200 Hz, the rotation speed did not influence the amplitude.
- For frequencies around 100 Hz, the amplitude of subsynchronous vibrations increased with the rotation speed.

The emergency shutdown (ESD) occurred when the vibration amplitude reached the trip alarm threshold, equal to 90 µm. When running at 210 Hz, the waterfall of the position showed clearly the presence of subsynchronous vibrations, mainly on the expander side. In addition, it has been noticed that the start-up procedure opening of inlet guide vanes (IGV) impacts the amplitude of subsynchronous vibrations. When the IGV is fully open, the subsynchronous vibrations are present but with much lower amplitude.

The first observation was the vibrations amplitude increased with the increase of rotational speed, and strongly depended on the process conditions as defined by the IGV.

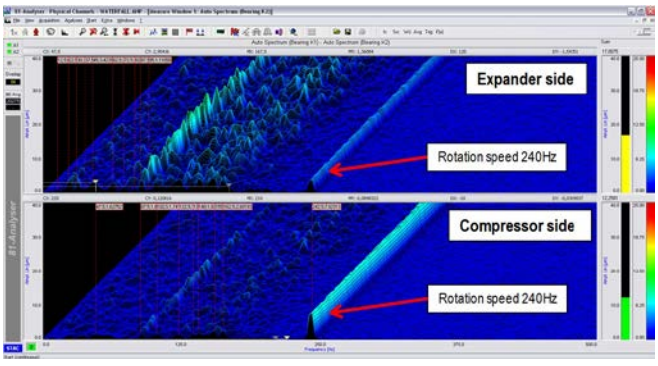

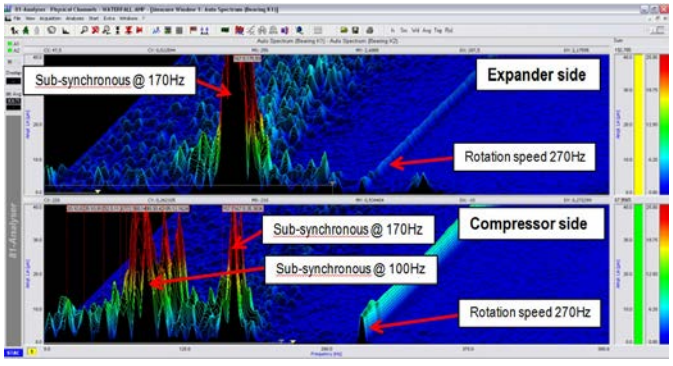

Figure 5: Left: When closing the IGV by 46%, Right: The vibrations increase leading to a trip

Below is the analysis performed on measurements done on May 2013. The temporal plot of the position showed:

- **Phase 1**: Before the trip, the machine was running at 255 Hz. Subsynchronous were limited to 40 µm, lower than the alarm level.
- **Phase 2**: High amplitude vibrations appeared just before the trip during 1.5 sec. Vibrations were only radial, and mainly on the expander side (VW13).
- **Phase 3**: During braking of the machine, vibrations appeared on the compressor side (VW24).

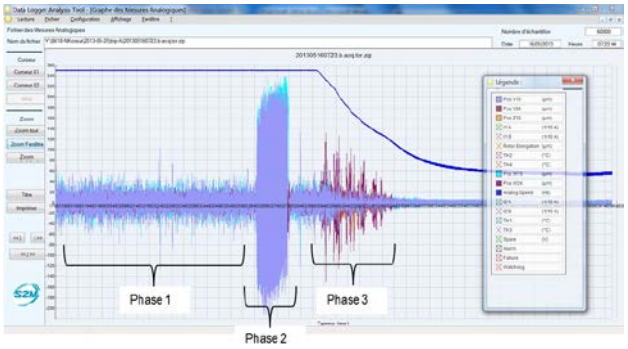

Figure 6: Temporal of the position (high sampling frequency data registered by the AMB controller)

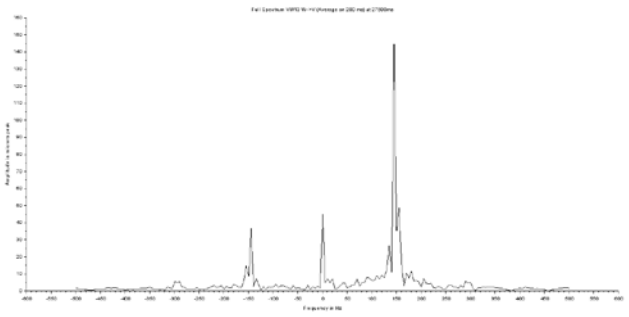

Figure 7: Spectrum of the position during the phase 2

The associated waterfall showed mainly forward harmonics, backward harmonics were low. Ploting precisely the position spectrum on expander side during the phase 2, main subsynchronous was at 150 Hz (amplitude close to trip). Backward harmonics at -150Hz had an amplitude of only 40 µm.

The orbit on the expander side during phase 1 was circular and with 40µm of amplitude (auxiliary bearing airgap is 150 µm). During the phase 2, the orbit was elliptic switching between the vertical axis and the horizontal axis.

The facts that the subsynchronous vibration at 150 Hz was around half the rotation speed and was mainly in forward mode, and the orbit was elliptic, were typical of fluid-induced NSV (Goldman and Muszynska, 1999). In fact, this phenomenon was very similar to oil whirl instabilities that may occur on a rotor-journal bearings/seals system under certain conditions. In case of oil-whirl, subsynchronous vibrations occur at frequencies of 30-60% of rotor rotational speed with a predominantly forward component. This is reflected in the full spectrum (Figures 8 & 9).

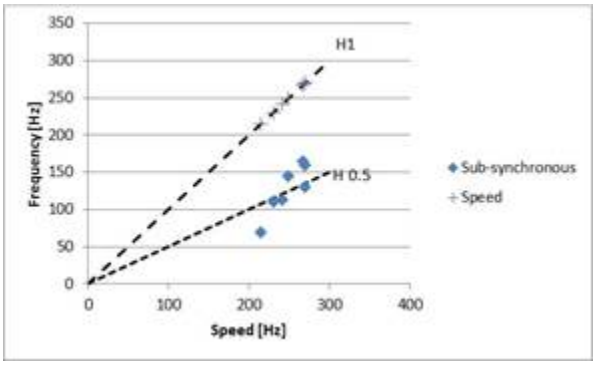

Figure 8: Subsynchronous frequency vs speed

The phenomenon is caused by fluid viscous forces and shearing effects in the rotor-stator gap. There are two components: fluid film radial force and a tangential force due to rotation and circumferential velocity. It leads to hydrodynamic cross-coupling destabilizing effects (i.e., appearance of skew-symmetric components in stiffness and damping matrices). In this case, it was likely to be caused by liquid fraction trapped in the front seal between the shroud and the casing and/or in the back wheel seal. Such destabilizing fluid-induced rotordynamic forces due to leakage in the gap between the impeller and shroud have been extensively studied by Caltex team (Brennen and Acosta, 2006). While more pronounced in the case of the AMB, note that this phenomenon is not strictly related to magnetic bearing machines but may happen in rotating turbomachines supported by conventional lube-oil bearings (Bentley, 2003).

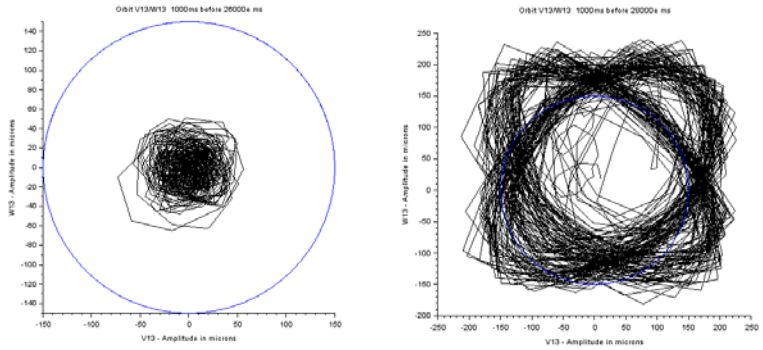

Figure 9: Subsynchronous frequency vs speed

These findings from the waterfall analysis, in addition to the following facts from the initial start-up attempts, proved that the existence of trapped liquid was the main source of the NSV:

- Increased temperature delayed the subsynchronous vibration appearance
- Increased outlet temperature also postponed the subsynchronous vibration
- Opening up nozzles during the initial start-up reduced the subsynchronous vibration amplitude

Figure 10 shows a typical phase diagram for a given gas. Most of the time typical process conditions for an expander are very close to or even directly on the dew point line. Depending on the inlet separator efficiency, the operating point could even be slightly in the two phase area.

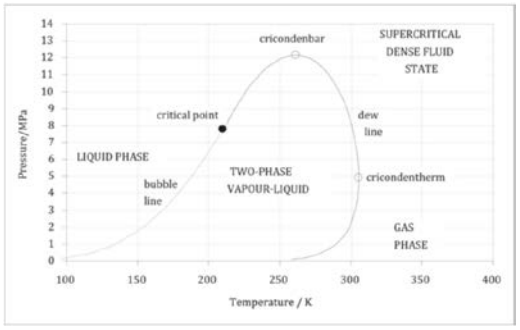

Figure 10: Typical phase diagram

For a given inlet pressure and assuming the gas composition is constant, the percentage of liquid in the inlet gas flow is directly linked to the inlet temperature (the lower the inlet temperature is, the higher the percentage of liquid is). This percentage of liquid will be increased once the gas goes through the inlet guide vanes (thermodynamic transformation through the IGV is described later on in this paper).

From a theoretical standpoint, because of the process inlet conditions on this unit during the start-up, the amount of liquids could be evaluated between 1 and 2.5% in weight. Nevertheless, due to the presence of the inlet separator, most of the liquid droplets were supposed to be removed from the gas upstream of the expander inlet itself.

There were two locations around the expander wheel where liquid could accumulate. As it can be seen on the following picture, a labyrinth was present at the backside of the impeller, and another labyrinth was present at the impeller shroud, between the expander cover and the follower (Figure 11).

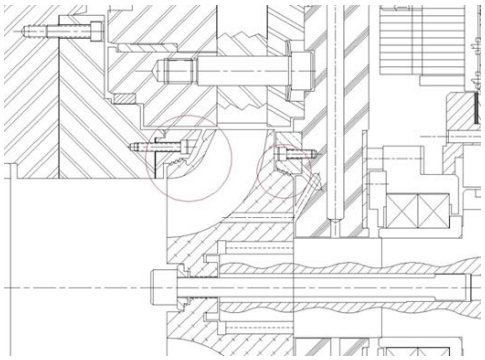

Figure 11: Possible locations for liquid entrapment

After it became clear that the liquid presence is causing the NSV, several attempts were performed to postpone this subsynchronous vibration further in order to enable the unit to run on higher speeds.

1. A vaporized methanol injection upstream of the turboexpander was one of the attempts which helped to run the unit up to 17,000 RPM. The unit ran steadily at this speed for several hours until the unit tripped because of a sudden spike on the expander bearing radial vibration which resulted from a sudden drop in the inlet temperature to -16°C.

2. Several software modifications of the AMB controller have been tried. Notably, the AMB stiffness was increased in the closed-loop transfer function in the low frequencies range. No significant improvement was achieved. Note that in this case, the room for maneuver is rather limited due to strong destabilizing cross-coupling effects at the wheel/labyrinth created by liquids on one hand, and bearings stiffness not sufficient to counterbalance the cross-coupling on the other hand. Hardware modifications were neither possible nor necessary.

3. Another attempt was to reduce the pressure drop across the nozzle. To do this, the unit was ramped up by manual adjustment of the upstream valve in a way to obtain 100% IGV opening at 13,000 RPM. After reaching 13,000 RPM, the inlet valve gradually opened and increased the speed. By this method, it was possible to delay the subsynchronous vibration appearance 4,000 RPM higher than when it was during the previous tests when nozzles were used to adjust the flow, allowing to speed up the machine to 18,000 RPM. It was possible to run the unit for 10 minutes at 18,000 RPM with no problem. Subsynchronous vibration started to appear on the waterfall diagram at around 18,200 RPM and finally tripped the unit at 18,400 RPM.

Expander Inlet Pressure (bar)	78.3	78.3	78.3	78.3	78.3	78.3	78.3	78.3	78.3
Expander Outlet Pressure (bar)	26.2	26.2	26.3	25.8	25.8	25.8	25.8	25.8	25.8
Pressure After Nozzles (bar)	37.4	37.7	38	38.3	38.4	38.6	38.8	38.9	38.9
IGV Position (%)	63.8	65.8	69.3	78.1	73.8	75.8	77.8	79.8	79.8
Speed (RPM)	16950	17120	17300	17560	17680	17680	17750	17950	17950

Table 2: Different configurations of pressure and IGV opening during start-up

4. To reduce the effect of the back wheel seal on induced instability, a swirl brake was added to the back wheel seal plate. The modified back wheel seal was installed on June 2013. For this start up, the manual IGV opening procedures were used to minimize the effect of the liquid's presence. At around 14,000 RPM, subsynchronous appeared at 97 Hz. When the speed reached 15,500 RPM it moved to 102 Hz and at 16,400 RPM it was sitting at 125 Hz and the unit tripped.

Figure 12: Back wheel seal with swirl brake

None of the above attempts was successful to bring the unit close to the operating speed. Since the gas composition and the operating conditions (pressure and temperature) could not be changed any further, the only option remaining to reduce the NSV caused by the trapped liquid, was to redesign the unit.

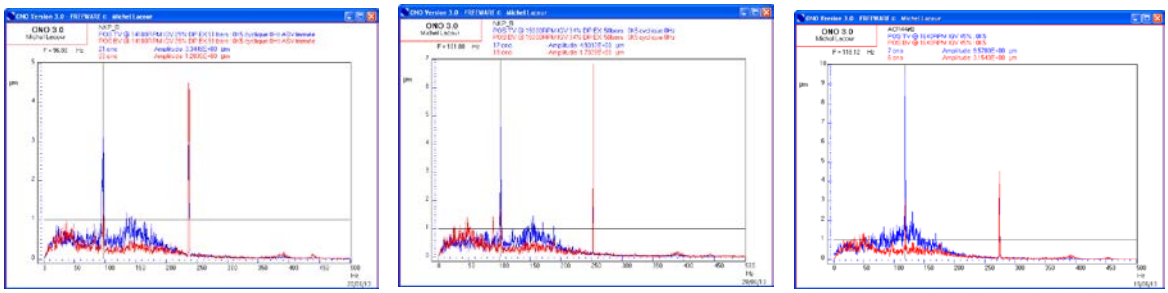

Figure 13: Left to right: 14,000 RPM, 15,500 RPM, 16,400 RPM

SECOND REDESIGN (OPEN WHEEL)

Open Wheel Design

On the second round of the redesign phase, a decision was made to completely remove one of the sources of the NSV. Adding a swirl brake to the back wheel seal was not successful and it was not possible to eliminate the back wheel seal completely as its removal would increase the net thrust force on the rotor assembly above the magnetic bearing thrust capacity. Therefore, a decision was made to completely remove the front seal by changing the closed wheel design to an open wheel. Moreover, there are some important differences in terms of rotordynamic fluid forces acting on closed and open impellers studied for turbopumps for rocket engines (Uchiumi et al., 2012). The effect of swirl brakes has been assessed by the same research group.

To reduce the impact on the redesign, the following notes were taken into consideration:

1. Keep the same weight and inertia
2. Obtain the same guaranteed efficiency points with an open wheel
3. Create high enough blade frequencies to avoid blade resonance without scarifying the area between the blades

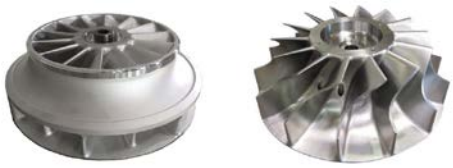

Figure 14: Open wheel vs closed wheel (shrouded) design

De-clamping System

Inlet guide vanes are too often neglected when an NSV issue affects an expander stage. Most of the documentation related to expander stage design does not refer to the thermodynamic conditions of the gas in the area between the nozzle exit and the expander impeller inlet. Jumonville, 2010, describes the basics for a proper expander stage design and insists on the importance of the IGV on the expander stage efficiency. This tutorial also describes the way the gas is flowing out of the IGV before entering the impeller itself.

Basic design rules for an expander stage are based on a 50% reaction degree. The static enthalpy drop through the complete expander stage is equally shared between the inlet guide vanes (IGV) on one side, and the impeller on the other side. The main goal of inlet guide vanes is to accelerate the gas flow, thus generating a uniform gas velocity and flow angle at the IGV exit. When operated at its design point, the ideal flow pattern should be such that the tangential velocity of the gas at the nozzle exit matches the impeller peripheral velocity. Gas is then flowing to the impeller with ideally a radial direction. When this match occurs, the expander is operated with U2/Co in the vicinity of 0.7.

However, during the transient phase, gas velocity at the nozzle outlet is significantly higher than during normal operation, with the nozzle being partially closed. The first consequence of this larger velocity exit impacts the reaction degree. Static enthalpy drop being more important in the nozzle group, the reaction degree is not anymore in the vicinity of 50%, but significantly lower. Because of this larger enthalpy drop, more condensates are generated through the IGV during those transient phases than during the normal operating cases.

The second consequence of this larger velocity exit impacts the flow gas pattern itself. Gas tangential velocity during those transient phases is significantly higher than the impeller tip speed. Therefore, the gas is not flowing anymore with a pure radial direction inside the impeller, but with some incidence. Due to the presence of liquid inside the gas, this incidence allows the liquid droplets in the gas path to be trapped in the labyrinth areas on the impeller itself (on both impeller sides with the original closed design, only at the expander back side with the open wheel redesign).

During the first stage of the redesign, it was noticed that by keeping the nozzles open during start-up, it was possible to postpone the subsynchronous vibrations inception. Ramping up the expander using a throttle valve upstream of the expander, and keeping the IGV fully open during the starting sequence minimizes the enthalpy drop through the IGV, and keeps the reaction degree of the expander stage in the vicinity of 50%, ensuring a radial gas flow inside the impeller.

In order to simulate the same effect during automatic IGV control at start-up and to partially control the liquid amount after nozzles and before the expander wheel, a de-clamping system was designed and added to the cold section of this unit. The main effect of the de-clamping system is to allow a portion of the flow to bypass the nozzles (flow between the nozzle faces and the nozzle rings). This de-clamping system is detrimental to the IGV efficiency. It impacts both the expander reaction degree, and the enthalpy drop through the IGV (both being somehow linked). Condensate generation upstream of the impeller is therefore minimized (because of the lower efficiency of the nozzles).

The de-clamping system was designed in a way to control the clamping force on the nozzles by changing the pressure applied to the nozzle surfaces. As shown in Figure 16, a port was added to the IGV assembly to connect the specific area on the nozzle clamping ring to two different sources of pressures. On one side, the port is connected to the expander inlet to be able to increase the pressure on nozzles and clamp the nozzles completely, and from the other side, the port is connected to the expander outlet to be able to reduce the pressure and de-clamp nozzles. Lowering the pressure on the nozzles provides the bypass flow to reduce the pressure drop across the nozzles.

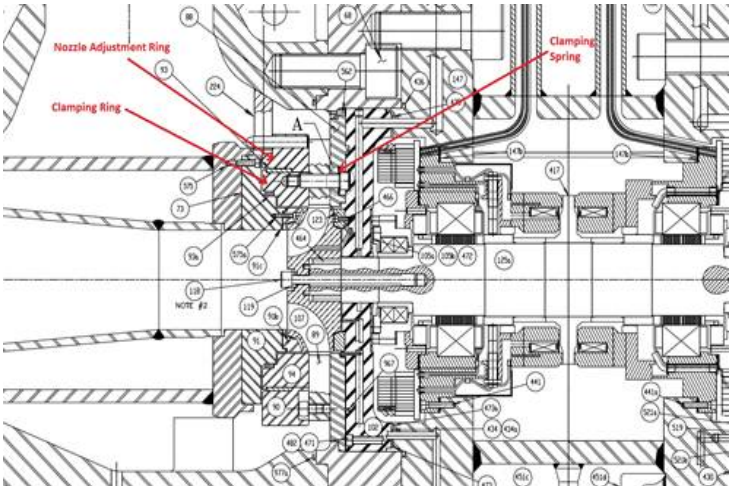

Figure 15: First redesign with no de-clamping system

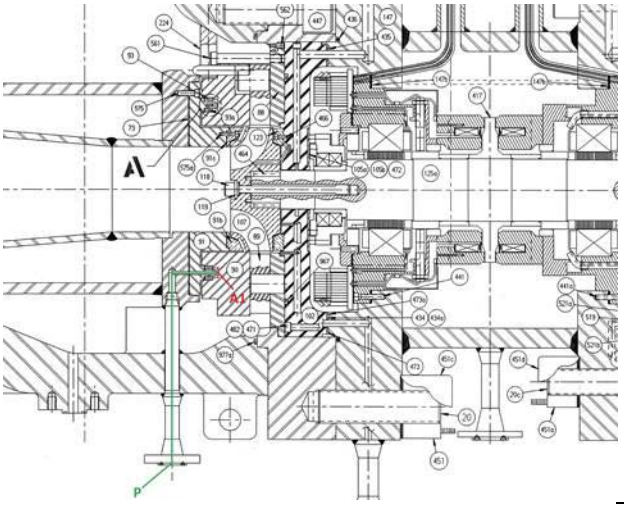

Figure 16: Second redesign with de-clamping system

Figure 17: De-clamping system after installation

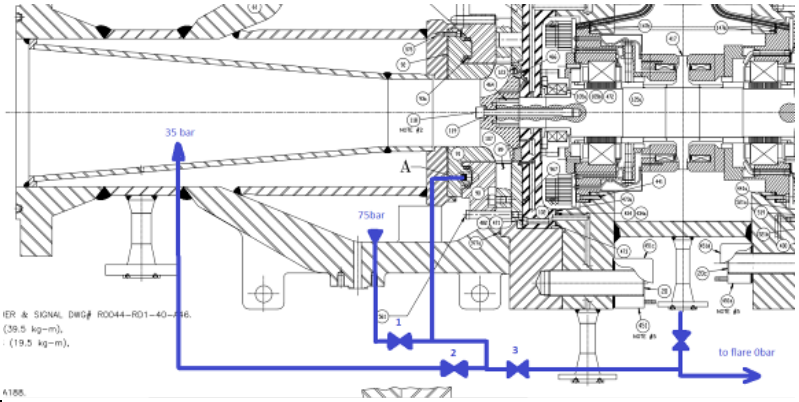

Figure 18: De-clamping system piping configuration

RESULTS

On May 2014, the open wheel design was installed on Unit B. During the start-up, the IGV control was set on automatic, the inlet temperature was -11°C, the nozzles were completely clamped (full pressure) and methanol injection was activated. The unit started up smoothly until it reached 11,000 RPM. At this point, subsynchronous vibration started to appear with much lower amplitude compared to the first redesign. As the speed further increased, the subsynchronous frequency and amplitude also increased to the point an alarm came up for an excessive radial vibration on the expander bearing but the unit did not trip. At this point, to observe the effect of the de-clamping system, the pressure on the nozzles was reduced by opening a valve connecting the nozzle clamping surfaces to the compressor outlet. As soon as the pressure reached less than 50 bar, the subsynchronous vibration started to fade out. Speed increased to 17,000 RPM and the subsynchronous vibration disappeared. The procedure started to clamp the nozzles back by increasing the pressure on the nozzles to above 62 bar and still no sign of subsynchronous frequencies appeared. The unit ramped up to the full speed of 20,500 RPM (not enough gas available to reach 21,000 RPM) with no problem. When the speed was reduced and the nozzles were clamped, the subsynchronous vibration appeared again close to 17,000 RPM and tripped the unit at around 16,500 RPM. The same speed reduction was tried when the nozzles were not clamped and no sign of subsynchronous vibration was observed down to 5,000 RPM.

It was obvious that subsynchronous frequencies appear between 11,000-17,000 RPM while the unit was clamped to the point it de-stabilized the unit. Subsynchronous frequency and its amplitude were a function of the speed while the unit was clamped and they both increased with the speed. The start-up procedure was revised (Figure 19) to indicate de-clamping the unit between 11,000-17,000 RPM. The same procedure was applied to the start-up of Unit A. The identical scenario that occurred with Unit B also happened with Unit A, and it was also possible to bring the unit to full speed (Figures 20 & 21).

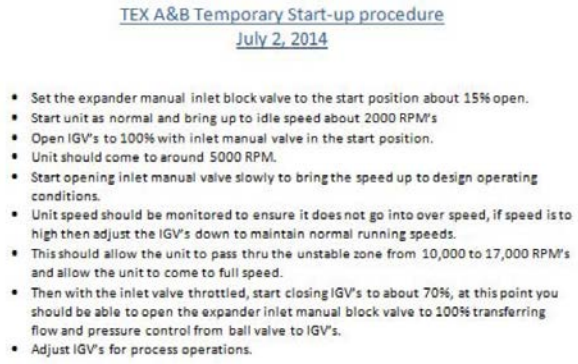
TEX A&B Temporary Start-up procedure
July 2, 2014

- Set the expander manual inlet block valve to the start position about 15% open.
- Start unit as normal and bring up to idle speed about 2000 RPM's
- Open IGV's to 100% with inlet manual valve in the start position.
- Unit should come to around 5000 RPM.
- Start opening inlet manual valve slowly to bring the speed up to design operating conditions.
- Unit speed should be monitored to ensure it does not go into over speed, if speed is to high then adjust the IGV's down to maintain normal running speeds.
- This should allow the unit to pass thru the unstable zone from 10,000 to 17,000 RPM's and allow the unit to come to full speed.
- Then with the inlet valve throttled, start closing IGV's to about 70%, at this point you should be able to open the expander inlet manual block valve to 100% transferring flow and pressure control from ball valve to IGV's.
- Adjust IGV's for process operations.

Figure 19: New start-up procedure

On Unit B, the subsynchronous vibration was totally removed as shown on the waterfall hereafter. On Unit A, there was still a remaining subsynchronous vibration around 25 Hz but with low amplitude (~20 µm). Despite these vibrations, the displacement amplitude was well below the threshold equal to 45 µm (0.3 x minimum gap) defined by API 617/ISO 14839-3 stability criteria as a safe operation zone. These subsynchronous vibrations did not impact the correct functioning of the machine.

With the new open wheel design and the de-clamping system, the two turboexpander units have run continuously at the full design speed (21,000 RPM) since May 2014.

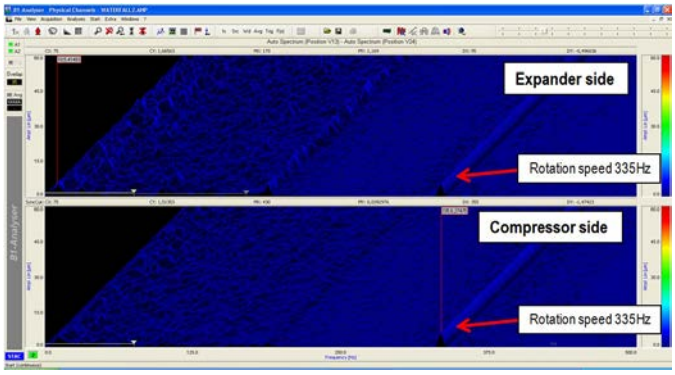

Figure 20: Unit B waterfall of the position

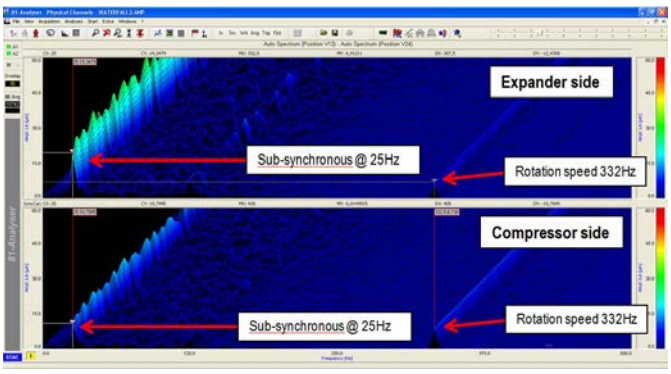

Figure 21: Unit A waterfall of the position

CONCLUSION

This lecture described how non-synchronous vibration (NSV) issues discovered at a very late stage were eventually solved. Four different aspects should be carefully reviewed and considered during the turboexpander design phase to avoid similar situations occurring.

Liquid presence is the first source for NSV and their consequences. Inlet separator upstream of the expander inlet shall therefore be carefully selected; especially the separation capacity shall not be affected when the expander is operated at partial load, or during start-up phase with reduced flow.

On the next step, expander impeller and the sealing design shall be carefully reviewed as well. Presence of liquid in the gas stream will impact expander behavior as liquid may accumulate between a rotating and a stationary part. An open impeller design seems to be a better choice for the expander which could be operated with a high amount of liquefied in the gas stream as it has one less sealing area in which liquid may be trapped. If a shrouded expander impeller design is the only design option, then the sealing areas needs to be designed in a way to avoid liquid gathering and be released back to the stream. Impeller disk design, labyrinth seal position and gap between the impeller disk and the casing are some of the parameters which could play a significant role in the NSV phenomena.

Nozzles are responsible for fifty percent of the process gas expansions. When a high amount of liquid is expected in the stream at the inlet of the expander case, the amount of liquid will increase significantly just after expansion at the nozzles and right at the OD of the wheel. This experiment proved that the amount of liquid at the OD of the wheel plays an even more important role than the amount of liquid at the inlet of the expander casing. So when a high amount of liquid is expected at the inlet during any operating condition, the recommendation is to implement a controllable system, like the de-clamping system described in this paper, to be able to adjust the expansion across the nozzles and thus be able to control the liquid amount at the wheel OD.

Finally, rotor dynamics with Active Magnetic Bearings (AMB) shall be carefully evaluated jointly with an AMB supplier, especially for operations at off-design conditions. Having the capacity to withstand subsynchronous excitation and maintain rotor radial vibration at an acceptable level will be beneficial to the expander operability. This, however, may depend on the nature and characteristics of the subsynchronous vibrations due to the external disturbances.

APPENDIX A

Redesign Gas Dynamic

Process Gas (Mol%):		M.W.										
Hydrogen	H2	2.0159										
Methane	C1	16.0430	82.5967	84.9842	81.3201	84.9790	82.5967	85.2454	81.3201	84.8606	82.5967	84.9842
Ethane	C2	30.0700	10.9158	11.5834	11.2310	11.7322	10.9158	11.4831	11.2310	11.7152	10.9158	11.5834
Propane	C3	44.0970	2.3028	0.8111	2.5478	0.6770	2.3028	0.6781	2.5478	0.7847	2.3028	0.8111
i-Butane	IC4	58.1230	0.3567	0.0423	0.4280	0.0335	0.3567	0.0305	0.4280	0.0460	0.3567	0.0423
n-Butane	NC4	58.1230	0.6130	0.0464	0.7697	0.0375	0.6130	0.0327	0.7697	0.0525	0.6130	0.0464
i-Pentane	IC5	72.1500	0.2056	0.0049	0.2950	0.0044	0.2056	0.0033	0.2950	0.0064	0.2056	0.0049
n-Pentane	NC5	72.1500	0.2239	0.0034	0.3289	0.0031	0.2239	0.0023	0.3289	0.0045	0.2239	0.0034
n-Hexane	NC6	86.1770	0.1964	0.0006	0.3393	0.0006	0.1964	0.0004	0.3393	0.0010	0.1964	0.0006
n-Heptane	NC7	100.2040	0.1053	0.0001	0.2083	0.0001	0.1053		0.2083	0.0001	0.1053	0.0001
n-Octane	C8	114.2310	0.0426		0.0916		0.0426		0.0916		0.0426	
C9	C9	128.2600	0.0065		0.0150		0.0065		0.0150		0.0065	
C10	C10	142.2850	0.0008		0.0019		0.0008		0.0019		0.0008	
Nitrogen	N2	28.0134	0.5928	0.6050	0.5768	0.6028	0.5928	0.6087	0.5768	0.6019	0.5928	0.6050
Oxygen	O2	31.9988										
Carbon Monoxide	CO	28.0100										
Carbon Dioxide	CO2	44.0100	1.8411	1.9186	1.8467	1.9298	1.8411	1.9154	1.8467	1.9271	1.8411	1.9186
Hydrogen Sulfide	H2S	34.0800										
Water / Steam	H2O	18.0153										
Air	AIR	28.9625										
Total:			100.0000	100.0000	100.0001	100.0000	100.0000	99.9999	100.0001	100.0000	100.0000	100.0000
Operating Condition												
UNIT			Exp	Comp	Exp	Comp	Exp	Comp	Exp	Comp	Exp	Comp
Tag No.			YE651 A/B	KB651 A/B	YE651 A/B	KB651 A/B	YE651 A/B	KB651 A/B	YE651 A/B	KB651 A/B	YE651 A/B	KB651 A/B
Condition			Re-Design		Off-Design		Off-Design		Off-Design		Off-Design	
Molecular Weight			19.73	18.55	20.30	18.53	19.73	18.48	20.30	18.57	19.73	18.55
Inlet	P1	(BAR A)	**79.0**	**24.0**	**79.00**	**24.00**	**79.0**	**24.0**	**79.0**	**24.0**	**79.0**	**24.0**
	T1	(C)	**-5.6**	**15.0**	**-11.20**	**15.00**	**-11.2**	**15.0**	**-5.6**	**15.0**	**-5.6**	**15.0**
Outlet	P2	(BAR A)	**26.0**	37.4	**26.00**	37.9	**26.0**	36.9	**26.0**	38.4	**26.0**	37.4
	T2	(C)	-55.7	51.6	-59.2	53.0	-59.9	50.7	-54.7	53.9	-55.7	51.6
Flow	(kg/hr)		**235736**	**212442**	**270471**	**215016**	**240584**	**211706**	**261948**	**212721**	**235736**	**212442**
	(lb/hr)		519704	468350	596280	474024	530391	466727	577491	468965	519704	468350
Delta Hs	(Btu/lbm)		33.55	24.25	31.87	25.15	31.95	23.65	33.38	25.79	33.55	24.25
ACFM	Inlet		1336	6233	1440	6318	1287	6237	1470	6235	1336	6233
	Outlet		3697	4510	4090	4523	3624	4554	4118	4423	3697	4510
Shaft Speed			21,000	21,000	21,300	21,300	20,740	20,740	21,500	21,500	21,000	21,000

REFERENCES

Agahi, R.R., Ershaghi, B., Baudelocque, L., 1995, "Turboexpanders with pressurized magnetic bearings for off-shore applications" *Proceedings of industrial conference and exhibition on applications of magnetic bearings, magnetic drives, and dry gas seals*, Alexandria, Virginia.

American Petroleum Institute, 2014, "API Standard 617, Eighth Edition, Axial and Centrifugal Compressors and Expander-Compressors," Washington, D.C., USA, API Publishing Services.

Bentley, D.E., 2003, *Fundamentals of Rotating Machinery Diagnostics,* ASME Press.

Bloch, H.P., Soare, C., 2001, *Turboexpanders and process applications*, Gulf Professional Publishing, Table 3-12, p. 81.

Brennen, C.E., Acosta, A.J., 2006, "Fluid-induced Rotordynamic Forces and Instabilities" *Journal of Structural Control & Health Monitoring*, 13(1), pp. 10-26.

Goldman, P., Muszynska, A., 1999, "Application of full spectrum to rotating machinery diagnostics", *Orbit*, pp.18-21.

ISO 14839-3:2006 Mechanical vibration – Vibration of rotating machinery equipped with active magnetic bearings – part 3: Evaluation of stability margin.

J. Jumonville, 2010, "Tutorial on Cryogenic Expanders", Proceedings of the 39th Turbomachinery Symposium.

Uchiumi, M.,Yoshida, Y., Nagao, N., Eguchi, M., 2012, "Comparison of Rotordynamic Fluid Forces Between Closed Impeller and Open Impeller", *Proceedings ASME 2012 Fluid Eng. Summer Meeting*, FEDSM 2012, July 8-12, Puerto Rico.

Valenchon, C. et al., 1995, The NKOSSA concrete oil production barge, *Proceedings of International Conference Offshore Mechanics and Arctic Eng*., Copenhagen, Denmark.

ACKNOWLEDGEMENTS

The authors wish to acknowledge the support and assistance of Askar Gubaidullin of SKF for his contribution and review.